


Human Umbilical Cord-Derived Mesenchymal Stem Cell Therapy Effectively Protected the Brain Architecture and Neurological Function in Rat After Acute Traumatic Brain Injury

Kuan-Hung Chen¹, Pei-Lin Shao², Yi-Chen Li³, John Y. Chiang^{4,5},
Pei-Hsun Sung³, Hui-Wen Chien², Fu-Yuan Shih⁶, Mel S. Lee⁷,
Wu-Fu Chen^{6,8,9,*}, and Hon-Kan Yip^{2,3,10,11,12,13,*} 

Cell Transplantation
Volume 29: 1–15
© The Author(s) 2020
Article reuse guidelines:
sagepub.com/journals-permissions
DOI: 10.1177/0963689720929313
journals.sagepub.com/home/ctl


Abstract

Intracranial hemorrhage from stroke and head trauma elicits a cascade of inflammatory and immune reactions detrimental to neurological integrity and function at cellular and molecular levels. This study tested the hypothesis that human umbilical cord-derived mesenchymal stem cell (HUCDMSC) therapy effectively protected the brain integrity and neurological function in rat after acute traumatic brain injury (TBI). Adult male Sprague-Dawley rats ($n = 30$) were equally divided into group 1 (sham-operated control), group 2 (TBI), and group 3 [TBI + HUCDMSC (1.2×10^6 cells/intravenous injection at 3 h after TBI)] and euthanized by day 28 after TBI procedure. The results of corner test and inclined plane test showed the neurological function was significantly progressively improved from days 3, 7, 14, and 28 in groups 1 and 3 than in group 2, and group 1 than in group 3 (all $P < 0.001$). By day 28, brain magnetic resonance imaging brain ischemic volume was significantly increased in group 2 than in group 3 ($P < 0.001$). The protein expressions of apoptosis [mitochondrial-bax positive cells (Bax)/cleaved-caspase3/cleaved-poly(adenosine diphosphate (ADP)-ribose) polymerase], fibrosis (Smad3 positive cells (Smad3)/transforming growth factor- β), oxidative stress (NADPH Oxidase 1 (NOX-1)/NADPH Oxidase 2 (NOX-2)/oxidized-protein/cytochrome b-245 alpha chain (p22phox)), and brain-edema/deoxyribonucleic acid (DNA)-damaged biomarkers (Aquaporin-4/gamma H2A histone family member X (γ -H2AX)) displayed an identical pattern to neurological

¹ Department of Anesthesiology, Kaohsiung Chang Gung Memorial Hospital and Chang Gung University College of Medicine

² Department of Nursing, Asia University, Taichung

³ Division of Cardiology, Department of Internal Medicine, Kaohsiung Chang Gung Memorial Hospital and Chang Gung University College of Medicine

⁴ Department of Computer Science and Engineering, National Sun Yat-sen University, Kaohsiung

⁵ Department of Healthcare Administration and Medical Informatics, Kaohsiung Medical University

⁶ Department of Neurosurgery, Kaohsiung Chang Gung Memorial Hospital and Chang Gung University College of Medicine

⁷ Department of Orthopedics, Kaohsiung Chang Gung Memorial Hospital and Chang Gung University College of Medicine

⁸ Department of Neurosurgery, Xiamen Chang Gung Hospital, Fujian, China

⁹ Department of Marine Biotechnology and Resources, National Sun Yat-sen University, Kaohsiung

¹⁰ Institute for Translational Research in Biomedicine, Kaohsiung Chang Gung Memorial Hospital

¹¹ Center for Shockwave Medicine and Tissue Engineering, Kaohsiung Chang Gung Memorial Hospital

¹² Department of Medical Research, China Medical University Hospital, China Medical University, Taichung

¹³ Division of Cardiology, Department of Internal Medicine, Xiamen Chang Gung Hospital, Fujian, China

* Both the authors contributed equally to this article

Submitted: February 15, 2020. Revised: April 20, 2020. Accepted: April 26, 2020.

Corresponding Authors:

Hon-Kan Yip, Division of Cardiology, Department of Internal Medicine, Kaohsiung Chang Gung Memorial Hospital and Chang Gung University College of Medicine, 83301, Kaohsiung.

Wu-Fu Chen, Department of Neurosurgery, Kaohsiung Chang Gung Memorial Hospital and Chang Gung University College of Medicine, 83301, Kaohsiung. Emails: han.gung@msa.hinet.net, chait@mail.cgmh.org.tw



Creative Commons Non Commercial CC BY-NC: This article is distributed under the terms of the Creative Commons Attribution-NonCommercial 4.0 License (<https://creativecommons.org/licenses/by-nc/4.0/>) which permits non-commercial use, reproduction and distribution of the work without further permission provided the original work is attributed as specified on the SAGE and Open Access pages (<https://us.sagepub.com/en-us/nam/open-access-at-sage>).

function among the three groups (all $P < 0.0001$), whereas the protein expressions of angiogenesis biomarkers (vascular endothelial growth factor/stromal cell-derived factor-1 α /C-X-C chemokine receptor type 4 (CXCR4)) significantly increased from groups 1 to 3 (all $P < 0.0001$). The cellular expressions of inflammatory biomarkers (cluster of differentiation 14 (+) cells (CD14+)/glial fibrillary acidic protein positive cells (GFAP+)/ a member of a new family of EGF-TM7 molecules positive cells (F4/80+)) and DNA-damaged parameter (γ -H2AX) exhibited an identical pattern, whereas cellular expressions of neural integrity (hexaribonucleotide Binding Protein-3 positive cells (NeuN+)/nestin+/doublecortin+) exhibited an opposite pattern of neurological function among the three groups (all $P < 0.0001$). Xenogeneic HUCDMSC therapy was safe and it significantly preserved neurological function and brain architecture in rat after TBI.

Keywords

traumatic brain injury, xenogeneic cell therapy, neurological function, inflammation, oxidative stress, apoptosis

Introduction

Strokes are classified into two major categories: ischemic and hemorrhagic. Different from ischemic stroke which is caused by interruption of blood supply to brain parenchyma, hemorrhagic stroke (HS) usually results from the rupture of a blood vessel or a vascular structural abnormality¹. Only about 13% to 20% of HS are due to hypertension of traumatic brain injury (TBI)². However, HS mortality is much higher than brain infarcts, with an estimated death rate of 26% to 30%³. Once severe neurological sequelae develop after cerebrovascular accident, the disability can cause huge social and familial economic burdens⁴. Current therapy for HS⁵ includes medical and surgical management. However, not every victim of HS is suitable for or can benefit from surgical intervention in clinical practice. Unfortunately, despite current standard method employed, it is estimated that more than 75% of stroke survivors suffered from disability, leading to decrease in their physical, mental, emotional, or a combination of these three essential elements. Their employability is also affected by more obvious neurological impairment⁶. Accordingly, finding a safe and effective way to salvage patients with intracranial hemorrhage (ICH) due to severe acute HS/TBI who are not candidate for neurosurgery is of utmost importance to patients and physicians.

The consequences of ICH⁷ include hematoma expansion, hydrocephalus, cerebral edema, and ischemia. Besides, the pathophysiologic mechanisms of HS-induced brain damage⁷ are mediated by apoptosis, necrosis, complement cascade and matrix metalloproteinases (MMP) activation, generation of reactive oxygen species (ROS), inflammatory reactions, inflammatory cell infiltration, and diverse expressions of molecular and cellular mediators. Accordingly, strategies that target against the inflammatory reaction, the generation and propagation of overwhelming immune responses, ROS, and oxidative stress, as well as molecular-cellular perturbations may have therapeutic potential for reducing HS-induced neuron death and brain dysfunction and improving neurological functional recovery. Additionally, strategies that elicit tissue/neuron regenerations (i.e., through intrinsic and extrinsic pathways)

would be of paramount importance for improving the neurological function and outcome after ICH.

Abundant data have shown that mesenchymal stem cells (MSCs) can inhibit inflammation and both innate and adaptive immunity through downregulating immunogenicity; they possess immunomodulatory function^{8,9} as well as have a great capacity for self-renewal by maintaining their multipotency and tissue regeneration^{10,11}. A review from Li et al.¹² demonstrated that human umbilical cord-derived MSC (HUCDMSC) therapy is advised to be an important candidate for allogenic cell treatment for ischemic stroke with unique “immunosuppressive and immunoprivilege” property. The potential therapeutic mechanisms comprise replacement of damaged neural cells, promotion of endogenous neural cells, secretion of neurotrophic factors, induction of vascularization and angiogenesis, reduction of apoptosis, and prevention of inflammatory effect¹³. However, the majority of MSC sources for TBI are derived from autologous or allogenic tissues which, therefore, cannot answer how reliable the immune privilege of the MSCs is^{14,15}. Additionally, genetic manipulation of the MSC prior to implantation has frequently used in reported studies thus raising another serious issue of tumorigenesis formation^{14,15}. These aforementioned issues show that xenogeneic source of HUCDMSC therapy for animals after TBI may provide stronger evidence to answer the above two concerns. However, a previous such study is only limited¹⁶. Importantly, the underlying mechanism of HUCDMSC therapy for improving the neurological function in animals after TBI has not been clearly investigated by the study¹⁶.

Interestingly, our recent studies^{17,18} have further demonstrated that not only was HUCDMSC therapy safe but it also effectively reduced brain infarct volume and preserved neurological function in rat after acute ischemic stroke as well as protected the heart against postheart transplant acute rejection in rodent. Accordingly, this study tested the hypothesis that HUCDMSC therapy effectively protected the brain integrity and neurological function in rat after TBI, especially focusing on investigation of the underlying mechanism involved in improvement of neurological function and presence or absence of tumorigenesis after HUCDMSC therapy. This result will encourage the use of HUCDMSC

for those patients with severe HS and who are unsuitable for surgical intervention.

Materials and Methods

Ethics

All animal procedures were approved by the Institute of Animal Care and Use Committee at Kaohsiung Chang Gung Memorial Hospital (Affidavit of Approval of Animal Use Protocol No. 2018102601) and performed in accordance with the Guide for the Care and Use of Laboratory Animals.

Animals were housed in an animal facility in our hospital approved by the Association for Assessment and Accreditation of Laboratory Animal Care International (Frederick, MD, USA), with free access to water and standard animal chow and temperature controlled at 24 C and 12-h light–dark cycles.

Traumatic Brain Injury Model by a Weight-Drop Device in Rat

Marmarou's weight-drop model was adopted for the rat model of TBI to induce ICH as previously described^{19–21}. In detail, animals in the three groups were anesthetized by inhalational 2.0% isoflurane (Rhodia Organique Fine Ltd., Bristol, UK.), placed supine on a warming pad (Riogo, USA) at 37°C, and then transferred to the weight-drop unit. A 1.5-cm-long midline scalp incision was used to expose the skull in each group of animals. The left frontal region (3 mm posterior to the coronal suture, 1.5 mm lateral to the midline) was selected as the impact region. A 200-g weight-drop device (a metal ball with 6 mm diameter) was released and dropped onto the left frontal bone from a 2.5-cm height. With this method, an impact velocity of 6 m/s and a dwell time of 150 ms (moderately severe injury) at an angle of 10° from the vertical plane produced an orthogonal impact with respect to the surface of the cortex. The scalp incision was then sutured. The sham group underwent the same procedure without the impact brain injury. The animals recovered from anesthesia in a portable animal intensive care unit (ThermoCare®, Daisy Products LLC, Paso Robles, CA, USA) for 24 h.

Although this method has been validated by previous studies^{19–21}, we still performed a pilot study to prove how consistent the brain injuries are from animal to animal. The results showed that the TBI with Marmarou's weight-drop model was quite comparable in the three animals (refer to supplemental Fig. 1). Accordingly, this method was confidently utilized in the present study.

Animal Grouping and Study Period

Pathogen-free, adult male (i.e., 10- to 12-wk old) Sprague-Dawley rats ($n = 30$) weighing 325 to 350 g (Charles River Technology, BioLASCO, Taipei, Taiwan) were randomly

categorized into three groups: sham-operated control (SC; group 1), TBI (group 2 + 3.0 cc culture medium), and TBI + HUCDMSC (1.2×10^6 cells by intravenous injection at 3 h after TBI; group 3). All animals were euthanized by day 28 after TBI procedure.

Our previous studies^{17,18} have found that intravenous administration of 1.2×10^6 adipose-derived mesenchymal stem cells (ADMSCs) was the suitable/optimal dose for effective protection of ischemia-related organ dysfunction. Based on the validation of this regimen, the dosage of HUCDMSC in the present study was, therefore, based on our previous studies^{17,18}. Four of the 10 animals in each group were utilized for assessment of the immunofluorescent (IF) staining. The remainder (i.e., $n = 6$ in each group) were utilized for western blotting.

Isolation and Characterization of HUCDMSCs

The procedures of isolation and culture were based on our previous report²². Briefly, the HUCDMSCs were provided by BIONET Corp. (Taipei City, Taiwan). The umbilical cords were collected, cut into small pieces, washed with phosphate-buffered saline (PBS) (Merck, USA), and then any contaminating blood and blood vessels removed. The small pieces were cultured in minimum essential medium eagle-alpha modification (alpha-MEM) (GIBCO, Grand Island, NY, USA) supplemented with 5% UltraGROTM (AventaCell, USA) and antibiotics (penicillin/streptomycin/amphotericin (PSA) antibiotics, GIBCO, Grand Island, NY, USA) to expand HUCDMSCs. Cells were replenished with fresh medium every 3 to 4 d at 37°C in a humidified atmosphere containing 5% CO₂. Umbilical cord MSCs were characterized by surface markers for flow cytometric analysis: cluster of differentiation (CD)13, CD14, CD29, CD31, CD34, CD44, CD45, CD73, CD90, human leukocyte antigen–DR isotype (HLA-DR), and CD105 (BD Pharmingen, San Diego, CA, USA). Additionally, umbilical cord MSCs possessed the differentiation probabilities of adipogenesis, osteogenesis, and chondrogenesis.

Brain Magnetic Resonance Imaging (MRI) Examination or Brain Hematoma/Brain Ischemic Volume (BIV)

The procedure and protocol for brain MRI have been described in our previous study²³. MRI was assessed on day 28 after TBI induction. Briefly, for MRI, rats were anesthetized by 3% inhalational isoflurane with room air and placed in an MRI-compatible holder (Biospec 94/20, Bruker, Ettlingen, Germany). MRI data were collected using a Varian 9.4T animal scanner (Biospec 94/20, Bruker) with a rat surface array. The MRI protocol consisted of 40 T2-weighted images. Forty continuous slice locations were imaged with a field-of-view of 30 mm × 30 mm, an acquisition matrix dimension of 256 × 256, and slice thickness of 0.5 mm. The repetition time and echo time for each fast spin-echo volume

were 4,200 and 30 ms, respectively. Custom software, ImageJ (1.43i, NIH, Bethesda, MD, USA), was used to process the region of interest. Planimetric measurements of images from MRI T2 were performed to calculate stroke volumes. Four of 10 animals in each group were randomly selected for brain MRI examination.

Corner Test for Assessment of Neurological Function

The sensorimotor functional test (Corner test; i.e., for detection of unilateral abnormalities of sensory and motor functions after stroke) was conducted for each rat at baseline and on days 3, 7, 14, and 28 after acute ischemic stroke (IS) induction as we previously described^{23,24}. Briefly, the rat was allowed to walk through a tunnel and then into a 60° corner. To exit the corner, the rat could turn either left or right. The results were recorded by a technician who was blind to the study design and treatment strategy. This test was repeated 10 to 15 times with at least 30 s between each trial. We recorded the number of right and left turns from 10 successful trials for each animal and used the results for statistical analysis.

Inclined Plane Test of Hind Limb Muscle Power and Coordination

To assess the muscle power and coordination of hind limbs of the rats, an inclined plane test (i.e., a measure of muscle tone and stamina) was adopted as previously described with slight modifications²⁵. In detail, during a 5-d period of acclimatization in a temperature- and humidity-controlled room with 12-h light–dark cycle and free access to water and standard animal chow, the rats were gently handled by laboratory personnel five times a day to let them be accustomed to human manipulation. In the following 3 d of training, the animals were placed on an inclined plane made of cardboard on which a horizontal friction trip provided a foothold for the animal's hind limbs as the inclination angle increased to prevent the animal from sliding down the slope. During the actual inclined plane test, each animal was placed on the inclined plane so that a secure foothold was established between the claws of its hind limbs and the friction trip. After confirmation of correct body position in the absence of anxious behavior and abnormally tense muscle tone of the animal, the inclination angle was slowly increased till the animal's hind limbs lost grasp of the friction trip and slid down the plane. The inclination angle was then recorded. After performing the experiment three times for each animal, the mean inclination angle was obtained by averaging the three recordings. The whole procedure was conducted by two independent technicians blinded to grouping of the animals. The quantitative data were expressed as means \pm SD. Intra-assay variability based on repeated measurement of the same animals was low

with a mean coefficient of variance of 3.2% study subjects.

Western Blot Analysis

The procedure and protocol for western blot analysis have been described in our previous studies^{17,18,23,24}. In detail, equal amounts (50 μ g) of protein extracts were separated by sodium dodecyl sulfate–polyacrylamide gel electrophoresis (SDS-PAGE). After electrophoresis, the separated proteins were transferred onto a polyvinylidene difluoride membrane (Amersham Biosciences, Amersham, UK). Nonspecific sites were blocked by incubation of the membrane in blocking buffer (5% nonfat dry milk in TBS containing 0.05% Tween 20) at room temperature for 1 h. Then the membranes were incubated with the indicated primary antibodies [endothelial nitric oxide synthase (1:1,000, Abcam, Cambridge, MA, USA), CD31 (1:1,000, Abcam), vascular endothelial growth factor (VEGF; 1:1,000, Abcam), stromal cell–derived factor (SDF)-1 α (1:1,000, Cell Signaling, Danvers, MA, USA), cleaved caspase 3 (1:1,000, Cell Signaling), cleaved-poly(adenosine diphosphate (ADP)-ribose) polymerase (PARP; 1:1,000, Cell Signaling), B-cell lymphoma (Bcl)-2 (1:1,000, Abcam), MMP-9 (1:3,000, Abcam), mitochondrial bax positive cells (Bax) (1:1,000, Abcam), Smad3 positive cells (Smad3) (1:1,000, Cell Signaling), Smad1/5 (1:1,000, Cell Signaling), hypoxia-induced factor-1 α (1:750, Abcam), and actin (1:10,000, Chemicon, Billerica, MA, USA)] for 1 h at room temperature. Horseradish peroxidase-conjugated antirabbit immunoglobulin G (IgG; 1:2,000, Cell Signaling) was used as a secondary antibody for 1-h incubation at room temperature. After washing, immunoreactive membranes were visualized by enhanced chemiluminescence (ECL; Amersham Biosciences) and exposed to Biomax L film (Kodak, Rochester, NY, USA). For quantification, ECL signals were digitized using Labwork software (UVP, Waltham, MA, USA).

Immunofluorescent Staining

The procedure and protocol of IF staining were based on our previous reports^{17,18,23,24}. In detail, for IF staining, rehydrated paraffin (GIBCO, Grand Island, NY, USA) sections were first treated with 3% H₂O₂ (GIBCO, Grand Island, NY, USA) for 10 min and incubated with Immuno-Block reagent (BioSB, Santa Barbara, CA, USA) for 30 min at room temperature. Sections were then incubated with primary antibodies specifically against gamma H2A histone family member X (γ -H2AX) (1:500, Abcam), VEGF (1:400, Abcam), and von Willebrand Factor (1:200, Merck Millipore, Taipei, Taiwan). Sections incubated with the use of irrelevant antibodies served as controls. Three sections of brain specimen from each rat were analyzed. For quantification, three randomly selected high power fields (HPFs) (200 \times or 400 \times for immunohistochemistry (IHC) and IF

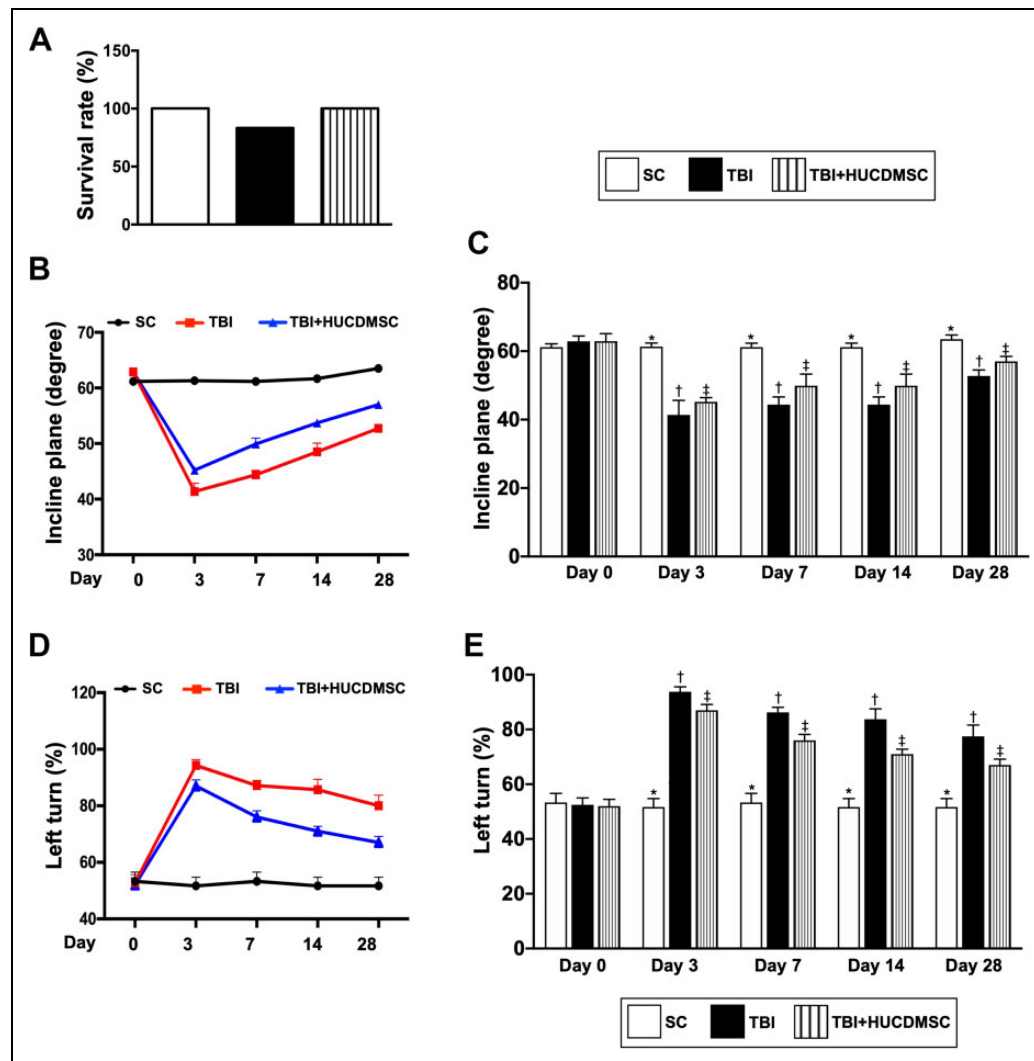


Fig. 1. The time courses of neurological function after TBI. (A) The mortality rate did not differ among the three groups, $P > 0.1$. (B) Illustrating the inclined plane test for determining limb motor function on days 0, 3, 7, 14, and 28 after acute TBI procedure. (C) Statistical analysis by day 0, $P = 1$. Statistical analysis by day 3 (*) vs. other groups with different symbols (†, ‡), $P < 0.001$. Statistical analysis by day 7 (*) vs. other groups with different symbols (†, ‡), $P < 0.001$. Statistical analysis by day 14 (*) vs. other groups with different symbols (†, ‡), $P < 0.001$. Statistical analysis by day 28 (*) vs. other groups with different symbols (†, ‡), $P < 0.001$. (D) Illustrating the corner test for determining limb motor function on days 0, 3, 7, 14, and 28 after TBI procedure. (E) Statistical analysis by day 0, $P > 0.5$. Statistical analysis by day 3 (*) vs. other groups with different symbols (†, ‡), $P < 0.001$. Statistical analysis by day 7 (*) vs. other groups with different symbols (†, ‡), $P < 0.001$. Statistical analysis by day 14 (*) vs. other groups with different symbols (†, ‡), $P < 0.001$. Statistical analysis by day 28 (*) vs. other groups with different symbols (†, ‡), $P < 0.001$. All statistical analyses were performed by one-way ANOVA, followed by Bonferroni multiple comparison post hoc test ($n = 10$ for each group). Symbols (*, †, ‡) indicate significance (at 0.05 level). ANOVA: analysis of variance; HUCDMSC: human umbilical cord-derived mesenchymal stem cell; SC: sham control; TBI: traumatic brain injury.

studies) were analyzed in each section. The mean number of positive-stained cells per HPF for each animal was then determined by summation of all numbers divided by 9.

Statistical Analysis

Quantitative data were expressed as means \pm SD. Statistical analysis was adequately performed by analysis of variance, followed by Bonferroni multiple comparison post hoc test. SAS statistical software for Windows version 8.2 (SAS

Institute, Cary, NC, USA) was utilized. A probability value < 0.05 was considered statistically significant.

Results

The Time Courses of Neurological Function After TBI

We first evaluated the mortality rate among the three groups during the study period and the result showed that the mortality rate did not differ among the three groups, that is, 0% (0/10) in group 1 versus 16.7% (2/12) in group 2 and 0% (0/10) in group

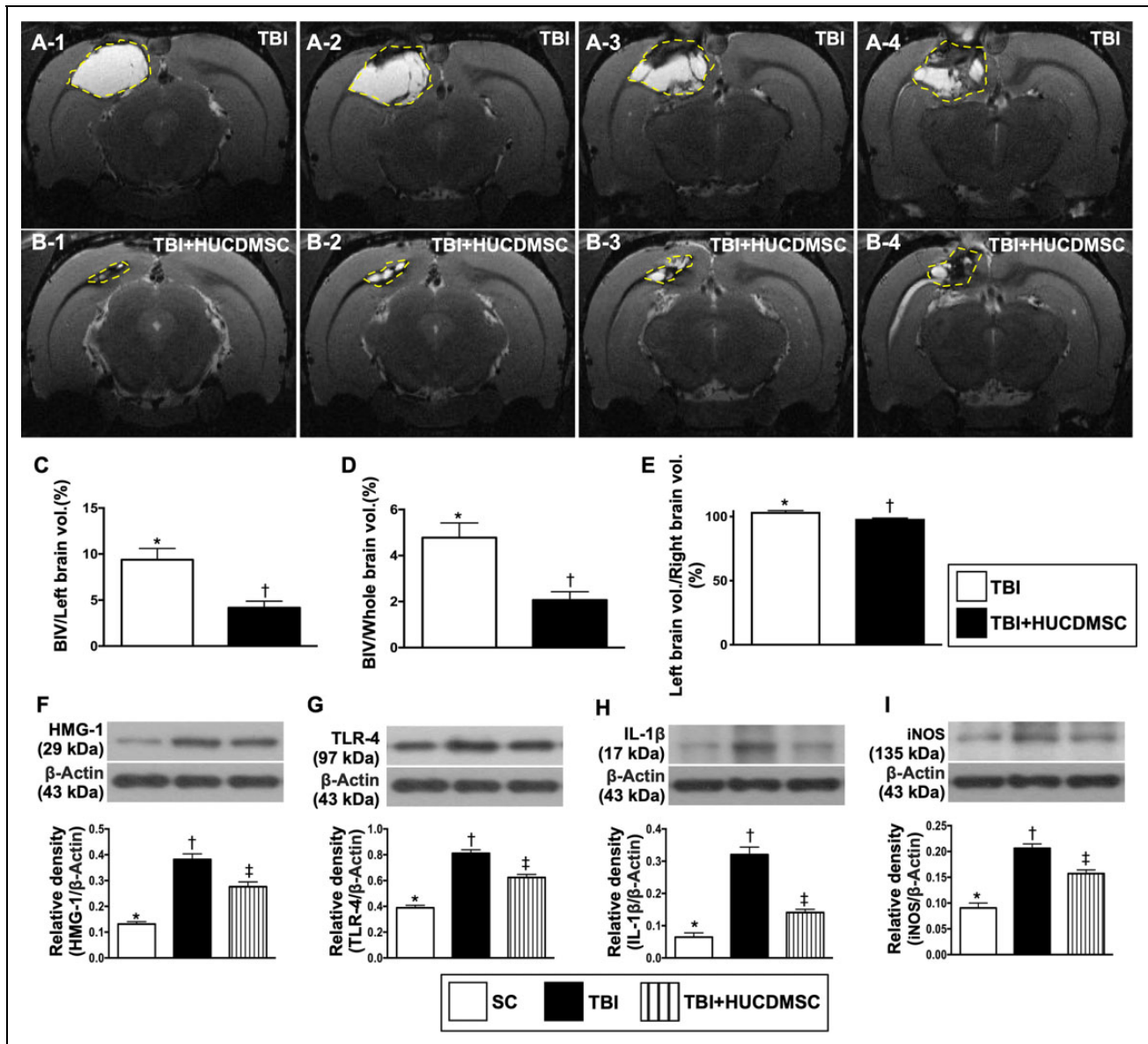


Fig. 2. Brain MRI findings and protein inflammatory biomarkers at day 28 after TBI induction. (A, B) Illustrating the brain MRI findings for identification of brain ischemic region (whitish color). The yellow dotted lines indicated the brain ischemic region. A-1 to A-4 indicated serial coronal sections of MRI findings in one TBI animal. B-1 to B-4 indicated serial coronal sections of MRI findings in one TBI animal treated by HUCDMSCs. (C) Analytical result of ratio of left brain ischemic volume (BIV) to left hemispheric brain volume by day 28 after TBI procedure ($n = 4$ for each group), * vs. †, $P < 0.001$. (D) Analytical result of ratio of left BIV to whole brain volume by day 28 after TBI procedure ($n = 4$ for each group), * vs. †, $P < 0.001$. (E) Analytical result of ratio of left brain volume to right brain volume by day 28 after TBI procedure ($n = 4$ for each group), * vs. †, $P < 0.001$. (F) Protein expression of high-mobility group protein I (HMG-1; *) vs. other groups with different symbols (†, ‡), $P < 0.001$. (G) Protein expression of toll-like receptor (TLR)-4 (*) vs. other groups with different symbols (†, ‡), $P < 0.001$. (H) Protein expression of interleukin (IL)-1 β (*) vs. other groups with different symbols (†, ‡), $P < 0.001$. (I) Protein expression of induced nitric oxide synthase (iNOS; *) vs. other groups with different symbols (†, ‡), $P < 0.001$. All statistical analyses were performed by one-way ANOVA, followed by Bonferroni multiple comparison post hoc test ($n = 4$ or 6 for each group). Symbols (*, †, ‡) indicate significance (at 0.05 level). ANOVA: analysis of variance; HUCDMSC: human umbilical cord-derived mesenchymal stem cell; MRI: magnetic resonance imaging; SC: sham control; TBI: traumatic brain injury; vol: volume.

3 ($P > 0.1$; Fig. 1A). Due to 2 rats were dead by day 10 after the procedure, 12 rats were used in group 2. For the purpose of 10 animals were required in each group for the complete follow-up of neurological functional test at the study period. Accordingly, totally 12 animals were utilized in group 2.

Next, the inclined plane test for determining limb motor function was performed for each rat at baseline and on days 3, 7, 14, and 28 after TBI induction (Fig. 1B, supplemental Table 2). On day 0, this parameter did not differ among the three groups (Fig. 1C). However, by days 3, 7, 14, and 28, this

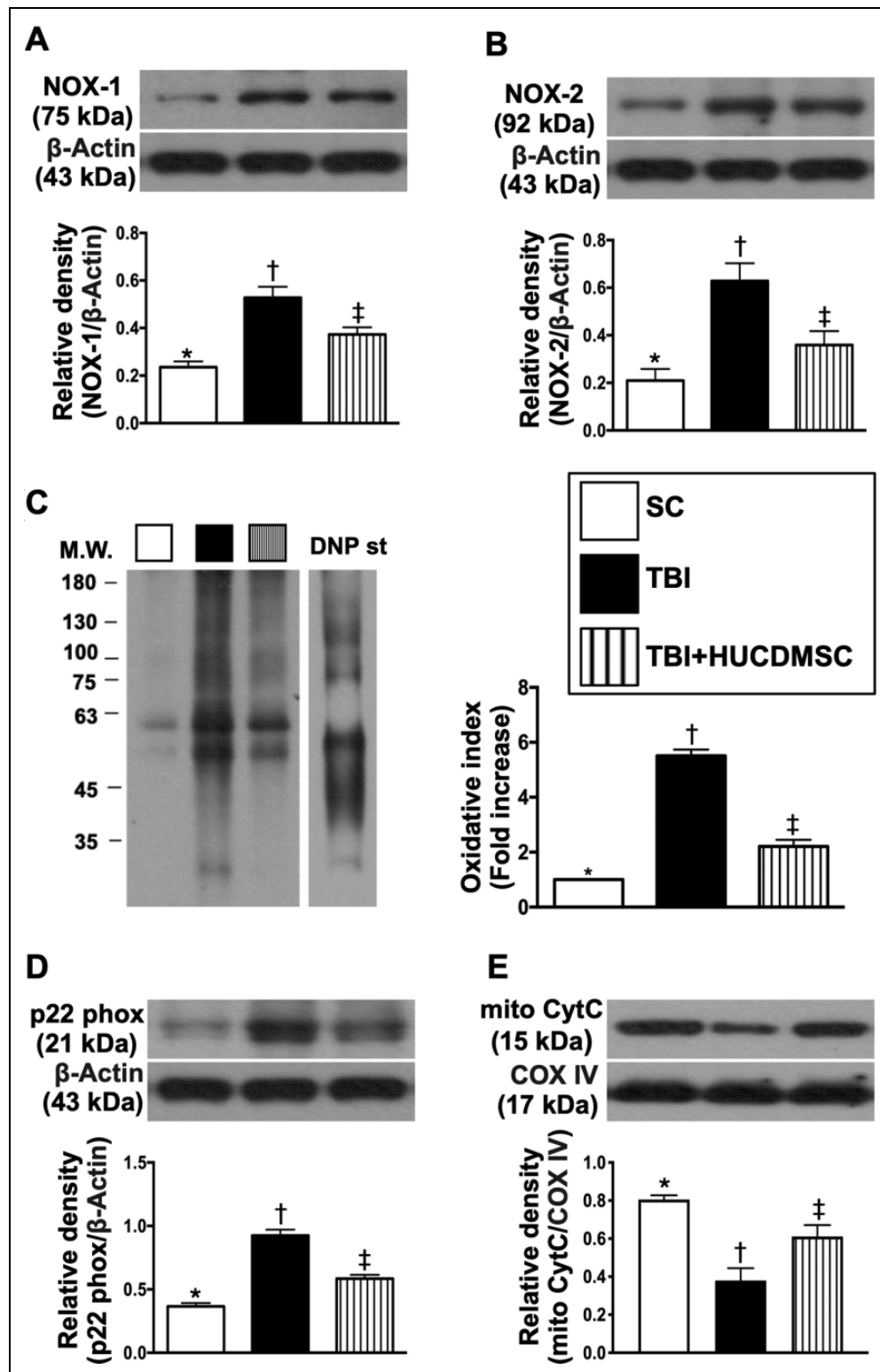


Fig. 3. Protein expressions of oxidative stress and mitochondrial damage by day 28 after TBI. (A) Protein expression of NOX-1 (*) vs. other groups with different symbols (†, ‡), $P < 0.001$. (B) Protein expression of NOX-2 (*) vs. other groups with different symbols (†, ‡), $P < 0.0001$. (C) Oxidized protein expression (*) vs. other groups with different symbols (†, ‡), $P < 0.0001$. (Note: Left and right lanes shown on the upper panel represent protein molecular weight marker and control oxidized molecular protein standard, respectively). (D) Protein expression of p22phox (*) vs. other groups with different symbols (†, ‡), $P < 0.001$. (E) Protein expression of mitochondrial cytochrome C (mit-Cyto-C; *) vs. other groups with different symbols (†, ‡), $P < 0.001$. All statistical analyses were performed by one-way ANOVA, followed by Bonferroni multiple comparison post hoc test ($n = 6$ for each group). Symbols (*, †, ‡) indicate significance (at 0.05 level). ANOVA: analysis of variance; DNP: 1,3-dinitrophenylhydrazone; HUCDMSC: human umbilical cord-derived mesenchymal stem cell; M.W.: molecular weight; NOX: NADPH Oxidase; SC: sham control; TBI: traumatic brain injury.

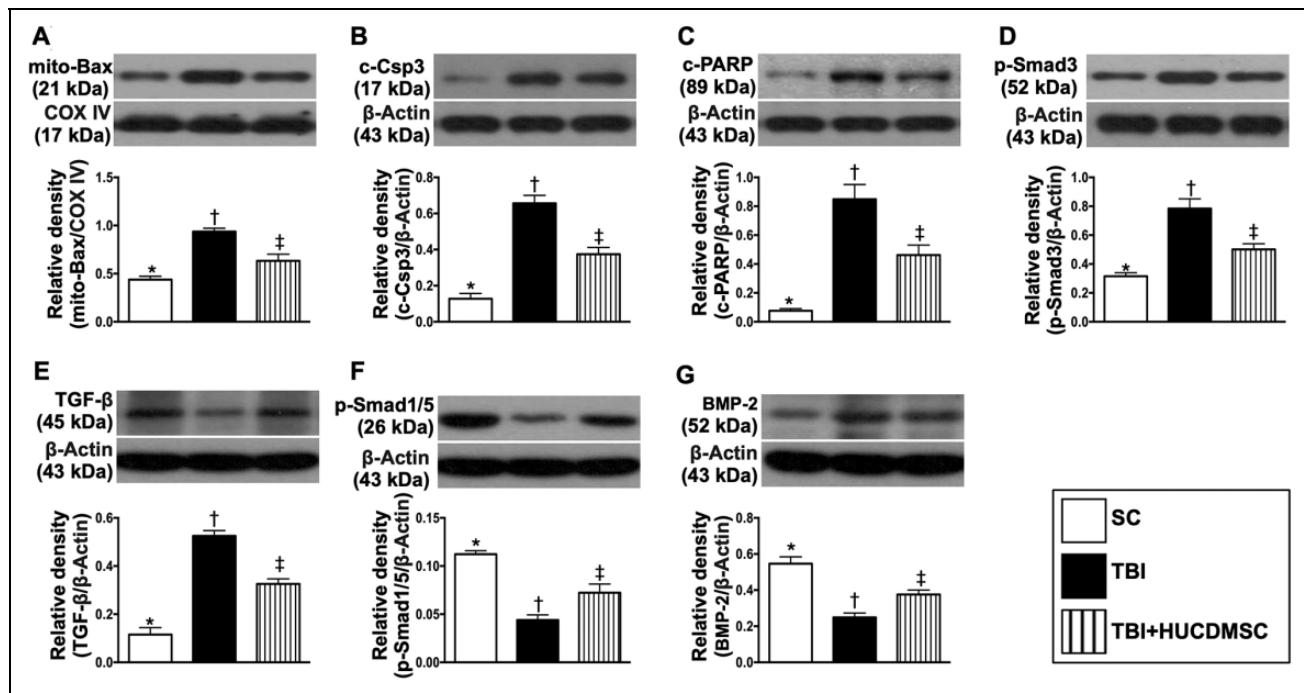


Fig. 4. Protein expressions of apoptotic, fibrotic, and antifibrotic biomarkers by day 28 after TBI. (A) Protein expression of mitochondrial (mito)-Bax (*) vs. other groups with different symbols (†, ‡), $P < 0.001$. (B) Protein expression of cleaved caspase 3 (c-Csp3; *) vs. other groups with different symbols (†, ‡), $P < 0.0001$. (C) Protein expression of cleaved-poly(ADP-ribose) polymerase (c-PARP; *) vs. other groups with different symbols (†, ‡), $P < 0.0001$. (D) Protein expression of Smad3 (*) vs. other groups with different symbols (†, ‡), $P < 0.0001$. (E) Protein expression of transforming growth factor (TGF)- β (*) vs. other groups with different symbols (†, ‡), $P < 0.0001$. (F) Protein expression of Smad1/5 (*) vs. other groups with different symbols (†, ‡), $P < 0.0001$. (G) Protein expression of bone morphogenetic protein (BMP-2; *) vs. other groups with different symbols (†, ‡), $P < 0.0001$. All statistical analyses were performed by one-way ANOVA, followed by Bonferroni multiple comparison post hoc test ($n = 6$ for each group). Symbols (*, †, ‡) indicate significance (at 0.05 level). ADP: adenosine diphosphate; ANOVA: analysis of variance; Bax: BCL2-associated X protein; DNP: 1,3-dinitrophenylhydrazine; HUCDMSC: human umbilical cord-derived mesenchymal stem cell; SC: sham control; Smad: Smad3 positive cells; TBI: traumatic brain injury.

parameter was significantly lower in group 2 than in groups 1 and 3, and significantly lower in group 3 than in group 1 (Fig. 1C).

Further, the sensorimotor functional test (Corner test) was performed for each rat at baseline and on days 3, 7, 14, and 28 after TBI induction (Fig. 1D). By day 0, the neurological function did not differ among the three groups (Fig. 1E). However, the Corner test indicated the attainment of a steady state of neurological functional impairment from days 3 to 28 following TBI procedure among groups 2 and 3 as compared with group 1 (Fig. 1E). A significant improvement in neurological function was found in group 3 as compared with group 2 by days 3, 7, 14, and 28 after TBI induction (Fig. 1E).

Measurement of BIV by Brain MRI and Protein Inflammatory Biomarkers on Day 28 After TBI Induction

To assess BIV, the brain MRI was performed for groups 2 and 3 by day 28 after TBI (Fig. 2: A1 to A4, B1 to B4). As expected, by day 28, the BIV was significantly

increased in group 2 than in group 3 (Fig. 2C–E), suggesting early administration of xenogeneic HUCDMSC to rodent was safe and also effectively protected the brain against TBI. Of importance was that no tumorigenesis was detected by brain MRI.

To clarify whether TBI would elicit prompt responses of inflammatory reaction, the western blot was examined. The results showed that the protein expressions of high mobility group box 1 protein (HMGB1)(Fig. 2F), toll-like receptor-4 (Fig. 2G), interleukin-1 β (Fig. 2H), and induced nitric oxide synthase (Fig. 2I), four indices of inflammatory biomarkers, were significantly increased in group 2 than in group 1, while significantly reduced in group 3, implicating that HUCDMSC therapy would notably suppress the inflammatory signaling.

Protein Expressions of Oxidative Stress and Mitochondrial Damage by Day 28 After TBI

To elucidate the protein level of oxidative stress, western blotting was conducted in the present study. As expected, the protein expressions of nicotinamide adenine dinucleotide

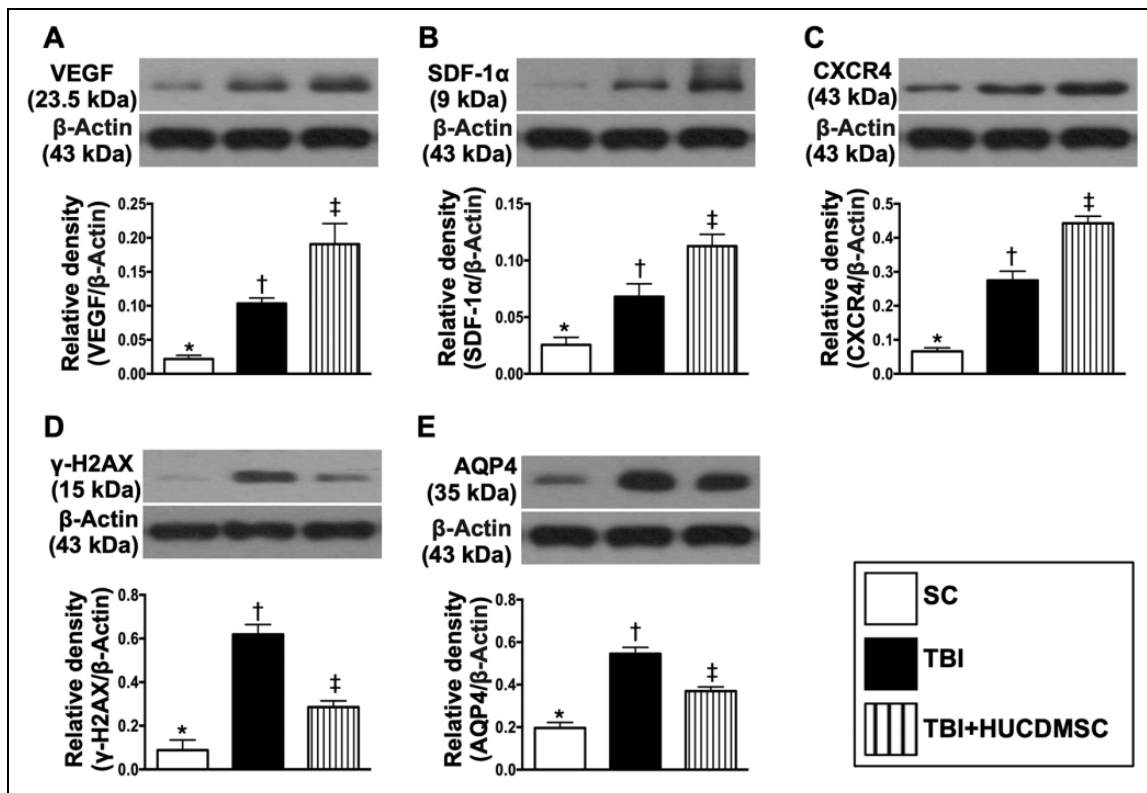


Fig. 5. Protein expressions of angiogenesis, brain edema, and deoxyribonucleic acid–damaged biomarkers by day 28 after TBI. (A) Protein expression of vascular endothelial progenitor cell (VEGF; *) vs. other groups with different symbols (†, ‡), $P < 0.0001$. (B) Protein expression of stromal cell–derived factor (SDF)-1 α (*) vs. other groups with different symbols (†, ‡), $P < 0.0001$. (C) Protein expression of CXCR4 (*) vs. other groups with different symbols (†, ‡), $P < 0.0001$. (D) Protein expression of γ -H2AX (*) vs. other groups with different symbols (†, ‡), $P < 0.0001$. (E) Protein expression of Aquaporin-4 (AQP4; *) vs. other groups with different symbols (†, ‡), $P < 0.001$. All statistical analyses were performed by one-way ANOVA, followed by Bonferroni multiple comparison post hoc test ($n = 6$ for each group). Symbols (*, †, ‡) indicate significance (at 0.05 level). ANOVA: analysis of variance; CXCR4: C-X-C chemokine receptor type 4; γ -H2AX: gamma H2A histone family member X; HUCDMSC: human umbilical cord–derived mesenchymal stem cell; SC: sham control; TBI: traumatic brain injury.

phosphate reduced form with the H ion (NADPH) Oxidase 1 (NOX-1) (Fig. 3A), NADPH Oxidase 2 (NOX-2) (Fig. 3B), and oxidized protein (Fig. 3C), three indicators of oxidative-stress biomarkers, were significantly higher in group 2 than in groups 1 and 3, and significantly higher in group 3 than in group 1. Consistently, the protein expression of cytochrome b-245 alpha chain (p22phox) (Fig. 3D), a membrane component of NADPH oxidase, displayed an identical pattern of NOX-1 among the three groups.

On the other hand, the protein expression of mitochondrial cytochrome C (Fig. 3E), an indicator of mitochondrial integrity, exhibited an opposite pattern of oxidative stress.

Protein Expressions of Apoptotic, Fibrotic, and Antifibrotic Biomarkers by Day 28 After TBI

Next, we performed the western blotting to determine the apoptotic and fibrotic protein levels in the brain ischemic region. The result showed that the protein expressions of mitochondrial Bax (Fig. 4A), cleaved caspase 3 (Fig. 4B), and cleaved PARP (Fig. 4C), three indices of apoptosis, were significantly higher in group 2 than in groups 1 and 3, and

significantly higher in group 3 than in group 1. Additionally, the protein expressions of p-Smad3 (Fig. 4D) and transforming growth factor (TGF)- β (Fig. 4E), two indicators of fibrosis, exhibited an identical pattern, whereas the protein expressions of p-Smad1/5 (Fig. 4F) and bone morphogenetic protein-2 (Fig. 4G), two indicators of antifibrosis, showed an opposite pattern of apoptosis among the three groups.

Protein Expressions of Angiogenesis, Brain Edema, and Deoxyribonucleic Acid (DNA)–Damaged Biomarkers by Day 28 After TBI

The protein expressions of VEGF (Fig. 5A), SDF-1 α (Fig. 5B), and C-X-C chemokine receptor type 4 (CXCR4) (Fig. 5C), three indices of angiogenesis factors, were significantly progressively increased from groups 1 to 3, suggesting an intrinsic response to ischemia that was enhanced by HUCDMSC therapy.

The protein expressions of γ -H2AX (Fig. 5D), a DNA-damaged biomarker, and Aquaporin-4 (Fig. 5E), a brain edema biomarker, were significantly increased in group 2

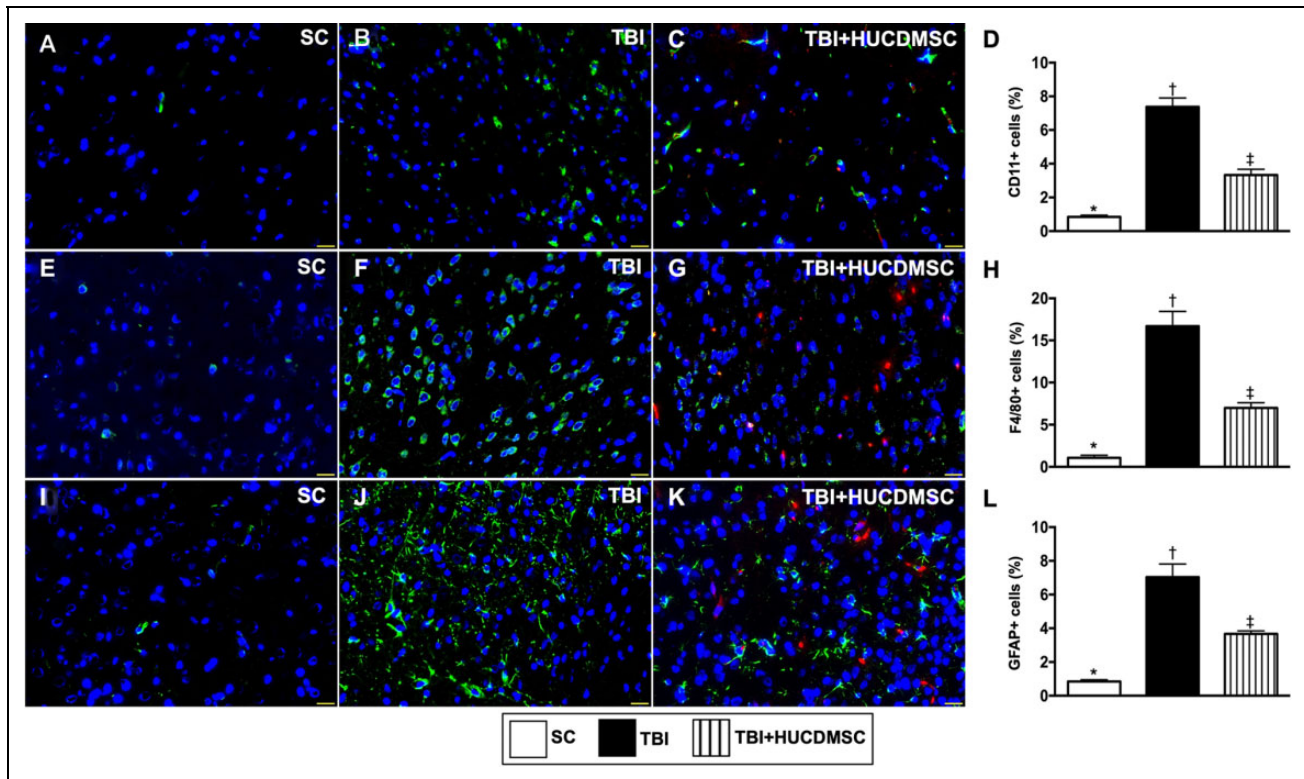


Fig. 6. Inflammatory cell expressions in brain ischemic zone by day 28 after TBI. (A–C) Illustrating the immunofluorescent (IF) microscopic finding (400 \times) for identification of cellular expression of CD11 (green color). Blue color indicated DAPI staining for identifying the nuclei. Red color in (C) indicated the implanted dye-tracking HUCDMSC and fragmentations. (D) Analytical results of the number of CD11+ cells (*) vs. other groups with different symbols (†, ‡), $P < 0.0001$. (E–G) Illustrating the IF microscopic finding (400 \times) for identification of cellular expression of F4/80 (green color). Blue color indicated DAPI staining for identifying the nuclei. Red color in (G) indicated the implanted dye-tracking HUCDMSC and fragmentations. (H) Analytical results of the number of F4/80+ cells (*) vs. other groups with different symbols (†, ‡), $P < 0.0001$. (I–K) Illustrating the IF microscopic finding (400 \times) for identification of cellular expression of glial fibrillary acid protein (GFAP; green color). Blue color indicated DAPI staining for identifying the nuclei. Red color in (K) indicated the implanted dye-tracking HUCDMSC and fragmentations. (L) Analytical results of the number of GFAP+ cells (*) vs. other groups with different symbols (†, ‡), $P < 0.0001$. Scale bars in right lower corner represent 20 μ m. All statistical analyses were performed by one-way ANOVA, followed by Bonferroni multiple comparison post hoc test ($n = 6$ for each group). Symbols (*, †, ‡) indicate significance (at 0.05 level). ANOVA: analysis of variance; CD: cluster of differentiation; DAPI: 4',6-diamidino-2-phenylindole; F4/80: a member of a new family of EGF-TM7 molecules positive cells; HUCDMSC: human umbilical cord-derived mesenchymal stem cell; SC: sham control; TBI: traumatic brain injury.

than in groups 1 and 3, and significantly increased in group 1 than in group 3.

Inflammatory Cell Expressions in Brain Ischemic Zone by Day 28 After TBI

The cellular expressions of CD11 (Fig. 6A–D), a member of a new family of EGF-TM7 molecules positive cells (F4/80) (Fig. 6E–H) and glial fibrillary acidic protein positive cells (GFAP) (Fig. 6I–L), three indicators of inflammation, were significantly higher in group 2 than in groups 1 and 3, and significantly increased in group 3 than in group 1.

Interestingly, even at day 28 after TBI, we still found abundant implanted HUCDMSCs (red-color dye-tracking; i.e., Fig. 6C, G, K) with intact morphology in the brain tissues, implicating that these cells still survived.

Cellular Expressions of DNA-Damaged and Neural Integrity Biomarkers in Brain Ischemic Zone by Day 28 After TBI

The cellular expression of γ -H2AX (Fig. 7A–D), a DNA-damaged marker, was significantly increased in group 2 than in groups 1 and 3, and significantly increased in group 3 than in group 1. On the other hand, the numbers of hexaribonucleotide Binding Protein-3 positive cells (NeuN+) (Fig. 7E–H), nestin+ (Fig. 7I–L), and doublecortin+ (Fig. 7M–P) cells, three indicators of neuron integrity, displayed an opposite pattern of γ -H2AX among the three groups. Again, by day 28 after TBI, abundant implanted HUCDMSCs (red-color dye-tracking; i.e., Fig. 7C, G, K) were observed by IF microscope with intact morphology in the brain tissues, once again implying that these cells still survived.

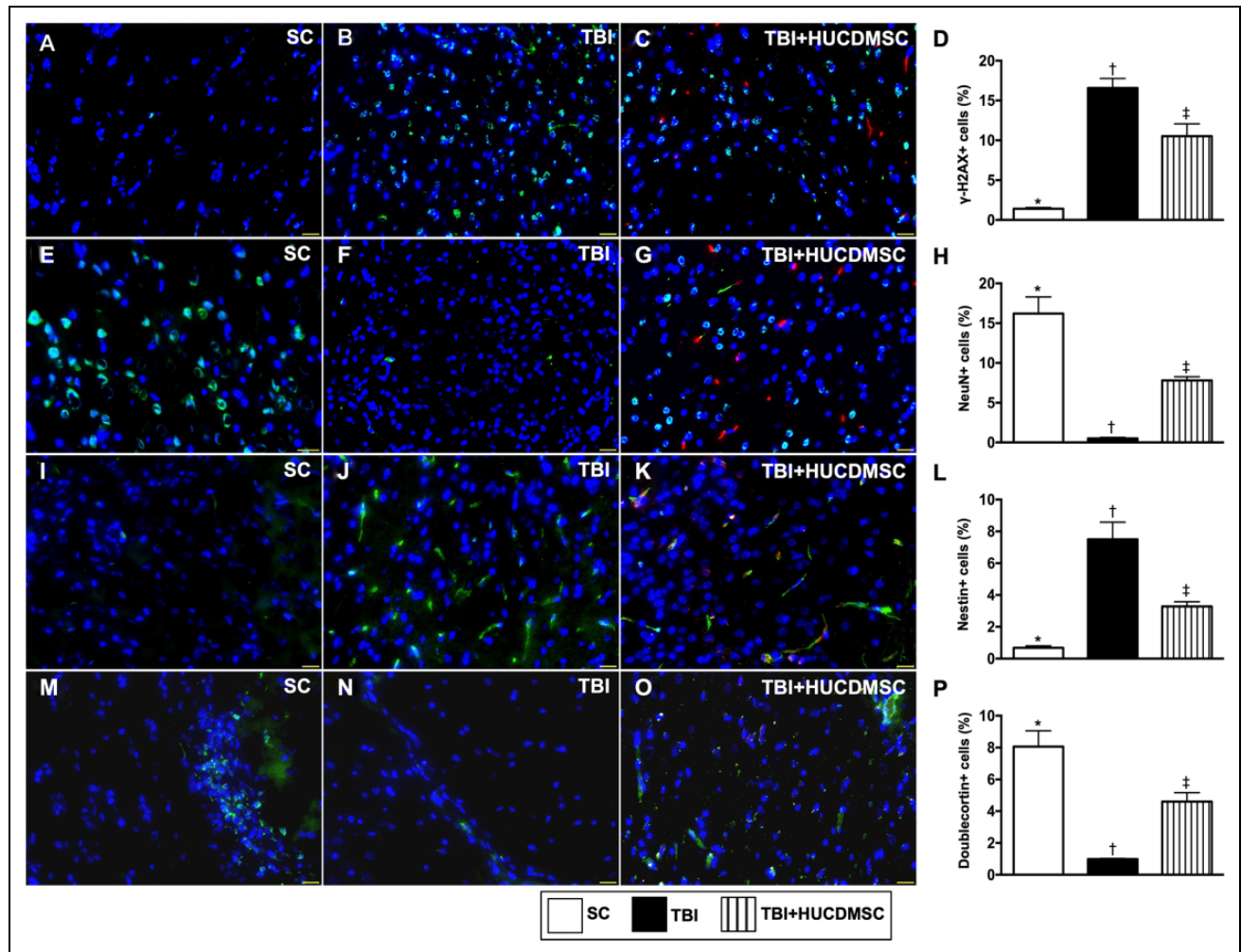


Fig. 7. Cellular expressions of deoxyribonucleic acid–damaged and neural integrity biomarkers in brain ischemic zone by day 28 after TBI. (A–C) Illustrating the immunofluorescent (IF) microscopic finding (400 \times) for identification of cellular expression of γ -H2AX (green color). Blue color indicated DAPI staining for identifying the nuclei. Red color in (C) indicated the implanted dye-tracking HUCDMSC and fragmentations. (D) Analytical results of the number of γ -H2AX+ cells (*) vs. other groups with different symbols ([†], [‡]), $P < 0.0001$. (E–G) Illustrating the IF microscopic finding (400 \times) for identification of cellular expression of NeuN (green color). Blue color indicated DAPI staining for identifying the nuclei. Red color in (G) indicated the implanted dye-tracking HUCDMSC and fragmentations. (H) Analytical results of the number of NeuN+ cells (*) vs. other groups with different symbols ([†], [‡]), $P < 0.0001$. (I–K) Illustrating the IF microscopic finding (400 \times) for identification of cellular expression of nestin (green color). Blue color indicated DAPI staining for identifying the nuclei. Red color in (K) indicated the implanted dye-tracking HUCDMSC and fragmentations. (L) Analytical results of the number of nestin+ cells (*) vs. other groups with different symbols ([†], [‡]), $P < 0.0001$. (M–O) Illustrating the IF microscopic finding (400 \times) for identification of cellular expression of doublecortin (green color). Blue color indicated DAPI staining for identifying the nuclei. (P) Analytical results of the number of doublecortin+ cells (*) vs. other groups with different symbols ([†], [‡]), $P < 0.0001$. Scale bars in right lower corner represent 20 μ m. All statistical analyses were performed by one-way ANOVA, followed by Bonferroni multiple comparison post hoc test ($n = 6$ for each group). Symbols (*, [†], [‡]) indicate significance (at 0.05 level). ANOVA: analysis of variance; DAPI: 4',6-diamidino-2-phenylindole; γ -H2AX: gamma H2A histone family member X; HUCDMSC: human umbilical cord–derived mesenchymal stem cell; NeuN: hexaribonucleotide Binding Protein-3 positive cells; SC: sham control; TBI: traumatic brain injury.

Discussion

This study which investigated the therapeutic impact of HUCDMSC on protecting the brain architecture and neurological function yielded several striking preclinical implications. First, HUCDMSC therapy was safe without any immunological side effect or tumorigenesis to the rodent. Second, HUCDMSC therapy significantly

improved the neurological functions and effectively protected the brain architecture against the TBI. Third, the results of this study showed that the underlying mechanisms of HUCDMSC therapy for improving the outcomes are mainly through inhibiting the inflammatory-immune and oxidative-stress reaction, augmenting the angiogenesis/restoring the blood flow and preserving the axonal/neural functional integrity (refer to Fig. 8).

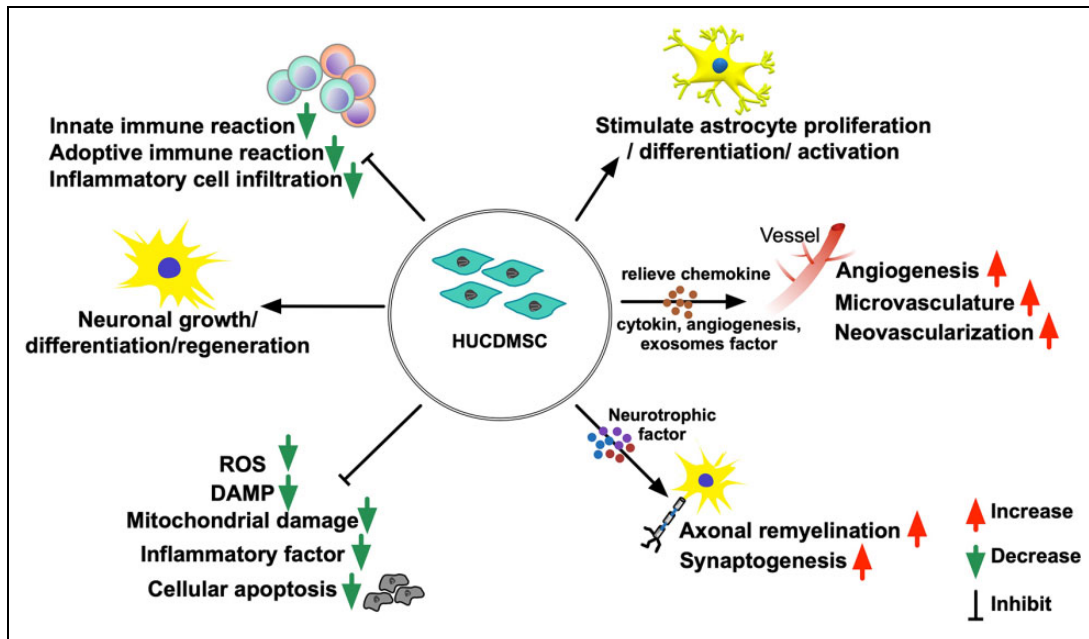


Fig. 8. The proposed schematic mechanism underlying the positive therapeutic effect of HUCDMSC on improving the outcome in TBI rat. DAMP: damaged associated molecular pattern; HUCDMSC: human umbilical cord–derived mesenchymal stem cell; ROS: reactive oxygen species; TBI: traumatic brain injury.

Our recent study¹⁷ has shown that HUCDMSC therapy effectively preserved the brain structural integrity and neurological function in rat after acute ischemic stroke. The most important finding in the present study was that the mortality rate of HUCDMSC-treated animals was 0% and the neurological function was notably improved in HUCDMSC-treated TBI animals than TBI-only counterparts. Additionally, by day 28 after TBI procedure, the brain MRI demonstrated that the BIV was substantially reduced in HUCDMSC-treated TBI animals than in TBI animals without treatment. Accordingly, our findings, in addition to corroborating our recent study¹⁷, could partially explain why the brain architecture and neurological function were markedly preserved in TBI animals after receiving HUCDMSC treatment.

Abundant data have demonstrated that MSCs act as a powerful inhibitor of inflammation and both innate and adaptive immunity through downregulating immunogenicity and possessing immunomodulatory function^{8,9,17,18}. Intriguingly, even in xenogeneic species of rodent, HUCDMSC therapy still has strong immunomodulatory capacity¹⁸, called “immunosuppressive and immunoprivilege” property¹². An essential finding in the present study was that the cellular and protein levels of inflammation and protein level of oxidative stress were significantly increased in TBI-only animals as compared with the SC. However, these molecular–cellular perturbations were substantially suppressed in TBI animals after receiving HUCDMSC therapy. Besides, the protein levels of the fibrotic, apoptotic, DNA/mitochondria-damaged biomarkers also corresponded to the

levels of inflammation and oxidative stress in the brain ischemic zone of TBI-only animals but were remarkably reversed in HUCDMSC-treated TBI animals. These findings, in addition to strengthening the results of previous studies^{8,9,12,17,18}, could once again explain why the HUCDMSC therapy effectively preserved the brain integrity and neurological function in TBI rats.

Plentiful data have revealed that MSCs maintained their multipotency and tissue regeneration^{10,11} and augmented angiogenesis/neovascularization^{17,25,26} as well as restored the blood flow in ischemic organs²⁷. Additionally, our previous study has further shown that ADMSC treatment enhanced the neurogenesis in rodent after acute ischemic stroke²⁸. A principal finding in the present study was that, as compared with TBI-only animals, not only the protein level but also the cellular level of angiogenesis biomarkers was remarkably increased in the TBI animals after receiving HUCDMSC therapy. Another principal finding in the present study was that the neurogenesis markers (i.e., NeuN+, nestin+, and doublecortin+ cells) were also substantially increased in TBI animals with than without HUCDMSC treatment. In this way, our findings, in addition to being consistent with the findings of previous studies^{10,11,17,25–28}, suggest that HUCDMSC therapy could restore the blood flow in ischemic area, resulting in tissues regeneration and neurogenesis.

Although the mortality rate did not differ among the groups (i.e., Fig. 1A), the neurological functional recovery was still severely impaired at day 28 after traumatic neurological function in TBI animals (refer to Fig. 1B, H) without than in those of TBI animals with HUCDMSCs

treatment. On the other hand, even underwent early HUCDMSCs treatment, the neurological function was still not total recover in these animals, highlighting that this neurological damage is permanent that raises the need to consider furthermore new innovative treatment for the TBI patients.

The kind of stem cells, the number of cells, and the route of stem cell administration have been well accepted as three key roles for successful improvement of organ dysfunction after cell therapy. Currently, both intravenous and intra-arterial administration of stem cells are commonly applied in either experimental studies^{29–32} or clinical trials^{33–35}. The advantage of intravenous administration of stem cells is that it is simple, early, and less noninvasive. However, quite a number of cells will be trapped in the lung, raising concern regarding the number of cells that could enter the target organ. On the other hand, the intra-arterial administration of stem cells in more invasive that sometimes it would need a guiding catheter for cell transfusion. In this way, surely, adequate numbers of cells would get into the target organ. Intriguingly, one previous study has established that intra-arterial delivery is not superior to intravenous delivery of stem cells in acute ischemic stroke in adult³⁶. In the present study, even by day 28 after TBI procedure, abundant intravenous administration of HUCDMSCs was observed in brain parenchyma. In this way, the previous findings support the result of the present study³⁶.

We mentioned in the introduction section that the possible molecular mechanism by which UCDMSCs are ameliorating the TBI is the mission of the present study. Undoubtedly, our results clearly displayed that the underlying mechanisms of HUCDMSC therapy for improving neurological function and the integrity of brain architecture are mainly through four independent signaling pathways: (1) inhibiting the inflammatory-immune reactions, (2) suppressing the generation of oxidative stress, (3) augmenting the angiogenesis/restoring the blood flow in brain region, and (4) preserving the axonal/neural functional integrity (Fig. 8).

Study Limitation

This study has limitations. First, although the short-term results (i.e., the study period was 28 d) were attractive and promising, the long-term prognostic outcome of HUCDMSC therapy in TBI rat remains uncertain. Second, the early time point of brain MRI was not performed as a “reference image” for comparison among the groups after TBI procedure and the effect of TBI and UCDMSCs transplantation on rodent memory was not assessed in the present study. Third, the dosage of HUCDMSC to be utilized in the present study was simply based on our previous studies^{14,15} without testing the efficacy of applying different dosages. Accordingly, this study was void of providing the optimal dosage of HUCDMSC for TBI therapy in rodent. Fourth, this study did not test whether single dosage is superior to multiple dosages or vice versa for improving the prognostic outcome in TBI

rodent. Finally, although extensive works had been done to the present study, the exact mechanism of action directly attributable to HUCDMSC was neither deeply investigated nor clearly identified.

In conclusion, the results of the present study proved that xenogeneic HUCDMSC therapy for TBI rat was safe and effectively protected the brain against TBI, resulting in preservation of the neurological function in rat.

Acknowledgments

We would like to give special thanks to BIONET Corp.Com for their support in GTP production of HUCDMSCs.

Ethical Approval

Ethical approval to report this case series was obtained from the Institute of Animal Care and Use Committee at Kaohsiung Chang Gung Memorial Hospital (Affidavit of Approval of Animal Use Protocol No. 2018102601).

Statement of Human and Animal Rights

All procedures in this study were conducted in accordance with the approved protocols of the Institute of Animal Care and Use Committee at Kaohsiung Chang Gung Memorial Hospital’s (Affidavit of Approval of Animal Use Protocol No. 2018102601).

Statement of Informed Consent

There are no human subjects in this article and informed consent is not applicable. HUCDMSC is a cell line.

Declaration of Conflicting Interests

The author(s) declared no potential conflicts of interest with respect to the research, authorship, and/or publication of this article.

Funding

The author(s) disclosed receipt of the following financial support for the research and/or authorship of this article: This study was supported by a program grant from Chang Gung Memorial Hospital, Chang Gung University (Grant No. BMRP542).

ORCID iD

Hon-Kan Yip  <https://orcid.org/0000-0002-6305-5717>

Supplemental Material

Supplemental material for this article is available online.

References

1. Donnan GA, Fisher M, Macleod M, Davis SM. Stroke. *Lancet*. 2008;371(9624):1612–1623.
2. Hu HH, Sheng WY, Chu FL, Lan CF, Chiang BN. Incidence of stroke in Taiwan. *Stroke*. 1992;23(9):1237–1241.
3. Hung TP. [Clinical aspects of cerebral hemorrhage]. *Taiwan Yi Xue Hui Za Zhi*. 1988;87(3):261–723.
4. Carlo DA. Human and economic burden of stroke. *Age Ageing*. 2009;38(1):4–5.
5. Masdeu JC, Rubino FA. Management of lobar intracerebral hemorrhage: medical or surgical. *Neurol*. 1984;34(3):381–383.

6. Paolucci S, Antonucci G, Grasso MG, Bragoni M, Coiro P, De Angelis D, Fusco FR, Morelli D, Venturiero V, Troisi E, Pratesi L. Functional outcome of ischemic and hemorrhagic stroke patients after inpatient rehabilitation: a matched comparison. *Stroke*. 2003;34(12):2861–2865.
7. Testai FD, Aiyagari V. Acute hemorrhagic stroke pathophysiology and medical interventions: blood pressure control, management of anticoagulant-associated brain hemorrhage and general management principles. *Neurol Clin*. 2008;26(4):963–985.
8. Engler AJ, Sen S, Sweeney HL, Discher DE. Matrix elasticity directs stem cell lineage specification. *Cell*. 2006;126(4):677–689.
9. Ryan JM, Barry FP, Murphy JM, Mahon BP. Mesenchymal stem cells avoid allogeneic rejection. *J Inflamm (Lond)*. 2005;2:8.
10. Franco Lambert AP, Fraga Zandonai A, Bonatto D, Cantarelli Machado D, Pegas Henriques JA. Differentiation of human adipose-derived adult stem cells into neuronal tissue: does it work? *Differentiation*. 2009;77(3):221–228.
11. Jiang Y, Jahagirdar BN, Reinhardt RL, Schwartz RE, Keene CD, Ortiz-Gonzalez XR, Reyes M, Lenvik T, Lund T, Blackstad M, Du J, et al. Pluripotency of mesenchymal stem cells derived from adult marrow. *Nature*. 2002;418(6893):41–49.
12. Li Y, Hu G, Cheng Q. Implantation of human umbilical cord mesenchymal stem cells for ischemic stroke: perspectives and challenges. *Front Med*. 2015;9(1):20–29.
13. Lee HS, Kim KS, Lim HS, Choi M, Kim HK, Ahn HY, Shin JC, Joe YA. Priming Wharton's jelly-derived mesenchymal stromal/stem cells with ROCK inhibitor improves recovery in an intracerebral hemorrhage model. *J Cell Biochem*. 2015;116(2):310–319.
14. Wu K, Huang D, Zhu C, Kasanga EA, Zhang Y, Yu E, Zhang H, Ni Z, Ye S, Zhang C, Hu J, et al. NT3(P75-2) gene-modified bone mesenchymal stem cells improve neurological function recovery in mouse TBI model. *Stem Cell Res Ther* 2019;10(1):311.
15. Shahrer RA, Linares GR, Wang Y, Hsueh SC, Wu CC, Chuang DM, Chiang YH, Chen KY. Transplantation of Mesenchymal stem cells overexpressing fibroblast growth factor 21 facilitates cognitive recovery and enhances neurogenesis in a mouse model of traumatic brain injury. *J Neurotrauma* 2020;37(1):14–26.
16. Wang Y, Peng D, Yang X, Huang P, Ye H, Hui Y, Wang X, Sun W, Wu H, Zhang S, Wang L, et al. Study on umbilical cord-matrix stem cells transplantation for treatment of acute traumatic brain injury in rats. *Turk Neurosurg* 2019;29(5):750–758.
17. Chen KH, Chen CH, Wallace CG, Yuen CM, Kao GS, Chen YL, Shao PL, Chen YL, Chai HT, Lin KC, Liu CF, et al. Intravenous administration of xenogenic adipose-derived mesenchymal stem cells (ADMSC) and ADMSC-derived exosomes markedly reduced brain infarct volume and preserved neurological function in rat after acute ischemic stroke. *Oncotarget*. 2016;7(46):74537–74556.
18. Yip HK, Lee MS, Sun CK, Chen KH, Chai HT, Sung PH, Lin KC, Ko SF, Yuen CM, Liu CF, Shao PL, et al. Therapeutic effects of adipose-derived mesenchymal stem cells against brain death-induced remote organ damage and post-heart transplant acute rejection. *Oncotarget*. 2017;8(65):108692–108711.
19. Feeney DM, Boyeson MG, Linn RT, Murray HM, Dail WG. Responses to cortical injury: I. Method local effects contusions in the rat. *Brain Res*. 1981;211(1):67–77.
20. Flierl MA, Stahel PF, Beauchamp KM, Morgan SJ, Smith WR, Shohami E. Mouse closed head injury model induced by a weight-drop device. *Nat Protoc*. 2009;4(9):1328–1337.
21. Xu J, Wang H, Ding K, Lu X, Li T, Wang J, Wang C, Wang J. Inhibition of cathepsin S produces neuroprotective effects after traumatic brain injury in mice. *Mediators Inflamm*. 2013;2013:187873.
22. Lee FY, Chen KH, Wallace CG, Sung PH, Sheu JJ, Chung SY, Chen YL, Lu HI, Ko SF, Sun CK, et al. Xenogeneic human umbilical cord-derived mesenchymal stem cells reduce mortality in rats with acute respiratory distress syndrome complicated by sepsis. *Oncotarget* 2017;8(28):45626–45642.
23. Chen YL, Tsai TH, Wallace CG, Chen YL, Huang TH, Sung PH, Yuen CM, Sun CK, Lin KC, Chai HT, et al. Intra-carotid arterial administration of autologous peripheral blood-derived endothelial progenitor cells improves acute ischemic stroke neurological outcomes in rats. *Int J Cardiol*. 2015;201:668–683.
24. Yuen CM, Chung SY, Tsai TH, Sung PH, Huang TH, Chen YL, Chen YL, Chai HT, Zhen YY, Chang MW, et al. Extracorporeal shock wave effectively attenuates brain infarct volume and improves neurological function in rat after acute ischemic stroke. *Am J Transl Res*. 2015;7(6):976–994.
25. Sheu JJ, Lee MS, Wallace CG, Chen KH, Sung PH, Chua S, Lee FY, Chung SY, Chen YL, Li YC, et al. Therapeutic effects of adipose derived fresh stromal vascular fraction-containing stem cells versus cultured adipose derived mesenchymal stem cells on rescuing heart function in rat after acute myocardial infarction. *Am J Transl Res*. 2019;11(1):67–86.
26. Chen YT, Sun CK, Lin YC, Chang LT, Chen YL, Tsai TH, Chung SY, Chua S, Kao YH, Yen CH, et al. Adipose-derived mesenchymal stem cell protects kidneys against ischemia-reperfusion injury through suppressing oxidative stress and inflammatory reaction. *J Transl Med*. 2011;9:51.
27. Leu S, Sun CK, Sheu JJ, Chang LT, Yuen CM, Yen CH, Chiang CH, Ko SF, Pei SN, Chua S, et al. Autologous bone marrow cell implantation attenuates left ventricular remodeling and improves heart function in porcine myocardial infarction: an echocardiographic, six-month angiographic, and molecular-cellular study. *Int J Cardiol*. 2011;150(2):156–168.
28. Leu S, Lin YC, Yuen CM, Yen CH, Kao YH, Sun CK, Yip HK. Adipose-derived mesenchymal stem cells markedly attenuate brain infarct size and improve neurological function in rats. *J Transl Med*. 2010;8:63.
29. Savitz SI, Misra V, Kasam M, Juneja H, Cox CS, Alderman S, Aisiku I, Kar S, Gee A, Grotta JC. Intravenous autologous bone

- marrow mononuclear cells for ischemic stroke. *Ann Neurol* 2011;70(1):59–69.
30. Misra V, Ritchie MM, Stone LL, Low WC, Janardhan V. Stem cell therapy in ischemic stroke: role of IV and intra-arterial therapy. *Neurology* 2012;79(13 Suppl 1): S207–S212.
 31. Chen KH, Chen CH, Wallace CG, Yuen CM, Kao GS, Chen YL, Shao PL, Chen YL, Chai HT, Lin KC, et al. Intravenous administration of xenogenic adipose-derived mesenchymal stem cells (ADMSC) and ADMSC-derived exosomes markedly reduced brain infarct volume and preserved neurological function in rat after acute ischemic stroke. *Oncotarget* 2016; 7(46):74537–74556.
 32. Vibhuti, Khan R, Sharma A, Jain S, Mohanty S, Prasad K. Intra-arterial transplantation of human bone marrow mesenchymal stem cells (hBMMSCs) improves behavioral deficits and alters gene expression in rodent stroke model. *J Neurochem* 2017;143(6):722–735.
 33. Bartolucci J, Verdugo FJ, Gonzalez PL, Larrea RE, Abarzua E, Goset C, Rojo P, Palma I, Lamich R, Pedreros PA, et al. Safety and efficacy of the intravenous infusion of umbilical cord Mesenchymal stem cells in patients with heart failure: a Phase 1/2 randomized controlled trial (RIMECARD Trial [Randomized Clinical Trial of Intravenous Infusion Umbilical Cord Mesenchymal Stem Cells on Cardiopathy]). *Circ Res* 2017; 121(10):1192–1204.
 34. Park EH, Lim HS, Lee S, Roh K, Seo KW, Kang KS, Shin K. Intravenous infusion of umbilical cord blood-derived Mesenchymal stem cells in Rheumatoid arthritis: a Phase Ia clinical trial. *Stem Cells Transl Med* 2018;7(9):636–642.
 35. Hammadi AMA, Alhimyari F. Intra-arterial injection of autologous bone marrow-derived mononuclear cells in ischemic stroke patients. *Exp Clin Transplant* 2019; 17(Suppl 1):239–241.
 36. Yang B, Migliati E, Parsha K, Schaar K, Xi X, Aronowski J, Savitz SI. Intra-arterial delivery is not superior to intravenous delivery of autologous bone marrow mononuclear cells in acute ischemic stroke. *Stroke* 2013;44(12): 3463–3472.